Received 3 August 2023; revised 1 October 2023; accepted 31 October 2023. Date of publication 3 November 2023; date of current version 4 December 2023.

Digital Object Identifier 10.1109/OJCOMS.2023.3330078

End-to-End Modelling and Simulation of NLOS Sub-6 GHz Backhaul via Diffraction for Internet Connectivity of Rural Areas

MUNEER M. AL-ZUBI (Member, IEEE), AND MOHAMED-SLIM ALOUINI (Fellow, IEEE)

Computer, Electrical, and Mathematical Science and Engineering Division, King Abdullah University of Science and Technology, Thuwal 23955, Makkah, Saudi Arabia

CORRESPONDING AUTHOR: M. M. AL-ZUBI (e-mail: muneer.zubi@kaust.edu.sa)

This work was supported by the KAUST Office of Sponsored Research.

ABSTRACT Many rural and remote areas around the world still lack access to the Internet due to the high deployment and maintenance costs, the lack of infrastructure, and the low income compared to urban regions. Therefore, cost-effective wireless backhaul links are required to connect these areas to the Internet core network. A wireless non-line-of-sight (NLOS) backhaul via diffraction in rural areas is a promising low-cost solution alternative to the traditional LOS backhaul. A reliable and cost-effective NLOS backhaul can be achieved if accurate propagation modelling and performance evaluation are performed before deployment. In this work, we first examine the accuracy of various terrain-based propagation models in predicting diffraction in different rural sites at unlicensed 5.8 GHz band. Although the classic irregular terrain model (ITM) is widely implemented in many radio frequency (RF) design software, we find that it overestimates the actual diffraction loss over small diffraction angles with an average error of −24 dB and RMSE value of 23 dB. However, a less complex rounded-obstacle diffraction model shows very high prediction accuracy compared to measured data with a negligible average error of −0.01 dB and RMSE value of 2.7 dB. Further, we evaluate the feasibility of an end-to-end NLOS backhaul link via simulation based on the IEEE 802.11ac standard using the practical characteristics of commercial RF equipment. The link performance is evaluated via end-to-end simulation in terms of the achieved throughput and the packet error rate (PER) over various antenna heights, modulation, and coding (MCS) schemes, and channel bandwidths. The results show that an NLOS backhaul at a distance of 11 km is viable with a throughput of 100-175 Mbps and PER of 0-0.1.

INDEX TERMS Backhaul, diffraction, microwave, non-line-of-sight, path loss, rural areas.

I. INTRODUCTION

ACCORDING to the International Telecommunication Union (ITU), 2.7 billion people in the world are still offline without Internet access and most of those live in developing countries and rural areas [1]. In addition to rural areas, today mobile broadband connectivity becomes a primary requirement for remote industrial camps and farms, e.g., oil and gas, mining, factory, etc., see Fig. 1. Backhaul links are required to connect these remote areas to the Internet core network. The available backhaul options are fiber optics, satellite, and point-to-point (PtP) wireless links. Among these options, PtP wireless backhaul is a flexible, quick-to-deploy, and cost-effective technology [2], [3]. However, other technologies are not economically viable in rural areas due to the low population, the complex terrain, and the lack of infrastructure, e.g., electricity and roads.

In modern mobile networks, PtP wireless communication connects millions of users to their networks and therefore, there is a critical demand for wireless backhaul infrastructures. Until today, the rule of thumb for designing and deploying conventional PtP wireless (microwave) links is the availability of a clear line-of-sight (LOS) path between the transmitting and receiving antennas. Furthermore, 60% of the first Fresnel zone should be clear of obstructions within the propagation path. In case of the absence of the LOS between the antennas, tall towers, repeaters, or passive reflectors are

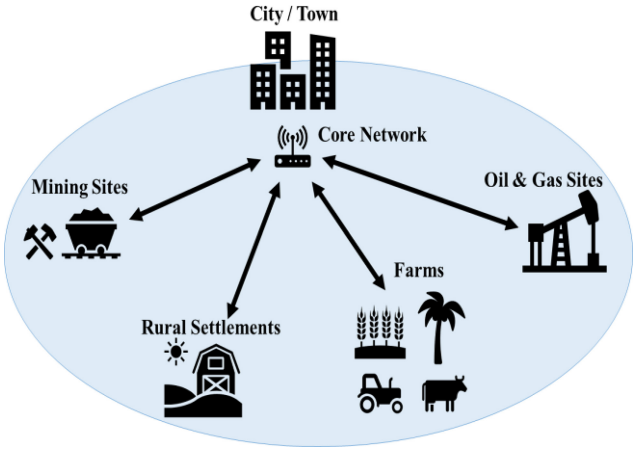

FIGURE 1. Examples of rural remote sites that require Internet connectivity.

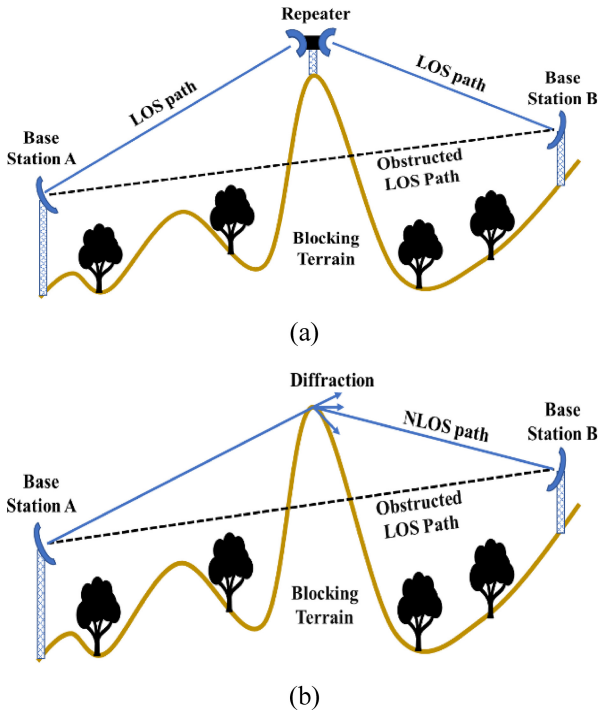

FIGURE 2. PtP NLOS wireless links between two base stations (BSs) using (a) repeater and (b) diffraction.

needed to overcome the blocked LOS path as shown in Fig. 2(a). Connecting a remote area to the Internet network may require many LOS backhaul links. However, this significantly increases the total deployment cost, including equipment, towers, maintenance, infrastructure, site lease, and site survey and planning. Thus, this option is not economically feasible for such rural and hard-to-reach areas.

Few works in the literature have considered the evaluation and modelling of non-line-of-sight (NLOS) PtP communication links at high frequency in rural areas. In [2], the performance of NLOS microwave backhaul links in small urban cells is examined via link and system-level simulations with experimental measurements at both 5.8 GHz and 28 GHz frequencies. The results show that an NLOS PtP microwave link at high frequency is a viable solution for wireless small-cell backhauling. In [4], the Log-distance path loss model is optimized for heterogeneous fixed wireless networks in rural environments based on measurements in rural regions of Canada. In [5], multi-hop Wi-Fi links for long backhaul connections in rural areas are examined via simulation which shows its feasibility as a cost-effective and practical solution for rural connectivity. A new rural macrocell (RMa) path loss model, namely, a close-in (CI) reference distance model, is developed based on 73 GHz millimeter wave measurements in rural areas which is more accurate than the existing 3GPP/ITU-R RMa path loss models and can be used for 0.5-100 GHz frequencies [6], [7].

An alternative approach for clear-LOS PtP wireless communication links is to exploit the NLOS links through the natural diffraction phenomena of electromagnetic (EM) waves, see Fig. 2(b). Diffraction is the bending of EM waves around the blocking obstacle that transfers some of the wave energy into the region of the geometrical shadow of the obstacle [8]. This approach can be used without changing the existing network architecture. Employing NLOS PtP wireless backhauling in rural areas will open new applications for microwave technology. This solution will eliminate the need for repeater sites and thus will significantly reduce the deployment and maintenance cost which is much higher in rural areas than urban regions due to the lack of infrastructure and the challenging terrain.

Recently, a research program supported by Facebook with partnerships of some universities and industry experts focused on carrying out radio frequency (RF) measurements and modelling of diffraction loss for NLOS microwave links over different terrains in rural areas [3], [9], [10]. Moreover, the authors present the feasibility of diffractive NLOS PtP links for broadband connectivity using a single obstacle with a shallow diffraction angle and modest/moderate foliage loss. This proposed solution has been implemented in carrier-grade networks in Peru by two mobile operators (Internet para Todos and Mayu Telecomunicaciones). In the same project, the feasibility and engineering-economic implications of a hybrid combination of LOS and NLOS links to build a practical and lower-cost networking solution are evaluated [10], [11].

The literature research is mostly focused on modelling the pathloss and evaluating the performance of high-frequency PtP NLOS communication systems in urban areas with less focus on rural areas, particularly evaluating the end-to-end performance in these environments. Utilizing the wireless NLOS links in rural regions requires an accurate prediction and modelling of the channel impairments in the propagation path. This step is critical in the design and planning phase to evaluate the performance of the PtP NLOS communication systems before the deployment. The main impairments in the NLOS propagation path at frequencies below 10 GHz (e.g., sub-6 GHz bands) in rural areas are the free space loss and the diffraction loss. It

is worth mentioning here that the diffraction represents the main propagation mechanism in this scenario. At these frequencies, the atmospheric conditions (e.g., attenuation due to rain and gases) are negligible [2]. Moreover, multipath fading is unlikely to occur in rural areas, particularly in case of the absence of the LOS path and narrow beam antennas are used [5]. It is important to realize the feasibility of a wireless communication system before the deployment phase. Therefore, it is essential to assess design parameters through theoretical modelling and simulation.

We present an end-to-end simulation and modelling framework for evaluating the propagation loss and the feasibility of PtP NLOS wireless backhaul at the sub-6 GHz frequency band based on the IEEE 802.11ac standard for Internet connectivity in rural and hard-to-reach areas. This work can help in the optimum planning and design of NLOS wireless backhauls via diffraction before deployment in rural areas. This will save time and cost, which is an important factor in low-income rural areas. Moreover, this work may give better insight into understanding of RF propagation and system performance in such propagation links. Thus, it may help improve the available RF propagation tools and models to accurately estimate the pathloss and evaluate the performance. The main contributions in this paper can be summarized as follows:

- Diffraction pathloss prediction in NLOS terrestrial backhaul systems has rarely been studied. Therefore, we first examine the accuracy of various terrain-based propagation models in the prediction of the diffraction loss in PtP NLOS propagation path over a single dominant blocking terrain and small diffraction angles in different rural sites. These models include the classic irregular terrain model (ITM), the modified ITM versions in Radio Mobile and Pathloss 5.0 software [12], [13], the rounded-obstacle diffraction model [14], the knife-edge diffraction model [14], and the terrain integrated rough earth model (TIREM^{TM}) [15], [16]. In order to make fair comparisons, a high-accuracy global space shuttle radar topography mission (SRTM) 1 arc-second is used as a primary digital elevation model (DEM) for all the propagation models under analysis [17]. The predicted results are verified with the measured data in rural sites at a frequency of 5.8 GHz found in [9].
- Although the classic Longley-Rice model, aka., the ITM (v1.2.2) model, is widely used in many RF propagation and design software, our results show an important conclusion about the sensitivity and inaccuracy of the classic ITM model under this propagation scenario based on comparison with experimentally measured data. We have shown that the classic ITM model significantly overestimates the actual pathloss in the propagation paths having a single dominant blocking terrain with near LOS and small diffraction angles at 5.8 GHz frequency. A similar fact was previously concluded in other works but for lower frequencies, i.e., in very high frequency (VHF) and ultra-high frequency (UHF) bands, which show that the ITM model does not work very well in the LOS mode and the early diffraction range [18], [19]. Therefore, the ITM model needs to be improved under these propagation conditions, since this model is widely implemented in many RF design computer software.
- We evaluated a more accurate model for this scenario using the rounded-obstacle diffraction model. We implement this model in MATLAB based on Recommendation ITU-R P.526 through a combination of a single knife-edge model and pathloss correction due to the radius of curvature of the blocking obstacle [14]. This model shows high prediction accuracy compared to the measured diffraction loss.
- We evaluate the feasibility of PtP NLOS wireless backhaul at 5.8 GHz in terms of throughput and packet error rate (PER) using an end-to-end simulation based on the predicted pathloss and the IEEE 802.11ac standard. The simulation is performed for various values of the antenna height, the modulation and coding scheme (MCS), and channel bandwidth (BW). We demonstrate that PtP NLOS wireless propagation through diffraction can provide reliable and low-cost backhaul solutions in rural areas. To make the simulation and modelling more realistic, we consider practical RF specifications for the RF transceiver similar to that of the commercial PTP550E unit from Cambium Networks designed based on IEEE 802.11ac standard and operating in frequency band 4.9 to 6.2 GHz.

The proposed approach can be mainly used to provide Internet connectivity to small settlements in rural and hard-to-reach areas where other backhaul options are not feasible as mentioned before. Connecting a radio access network (RAN) in a remote rural area to the Internet core network may require multiple backhaul links and repeaters due to mountains and obstacles. In the current conventional deployment of microwave backhauls, the path between any two base stations should be a clear LOS, otherwise, repeaters must be installed. However, using this hybrid approach by replacing some LOS links with diffractive NLOS links will reduce the total number of intermediate repeaters required. Many repeaters can be connected using mesh topology to provide Internet connectivity for many users and settlements. The users can connect their equipment such as cell phones and computers to the RAN at the destination through a wireless or wire technology such as 4G LTE, 5G, Ethernet, etc. This will reduce the deployment and maintenance cost of building new sites including the cost of RF equipment, towers, power supply sources, transportation costs, land lease, network planning costs, and regular maintenance. In fact, the deployment cost is higher in rural and remote areas compared to urban regions due to lack of infrastructure and challenging terrain.

In this work, the system is analyzed for the unlicensed frequency band (5.8 GHz), but it is expected to work with the

licensed band (6 GHz) as both frequencies are close to each other. Using long-distance plug-and-play PtP microwave platforms based on wireless local area network (WLAN) standards can reduce the cost of deployment which is a critical factor for rural areas. Although the advancements in IP microwave technology are mostly driven by high throughput demands in urban areas, it is practically and economically feasible for connectivity of rural areas.

This article is organized as follows. In Section II, we present the terrain-based radio propagation model used to predict the pathloss. The end-to-end wireless communication system is illustrated in Section III. In Section IV, we show and discuss the theoretical and simulation results. Finally, the paper is concluded in Section V.

II. RADIO PROPAGATION PATH LOSS MODELS

A. PATH LOSS AND LINK BUDGET

This subsection provides an overview of RF path loss prediction and link budget calculation considering the power gains and losses experienced by radio waves between the transmitter and the receiver. In a real-world propagation channel, the transmitted radio signal is affected by various factors in the radio propagation path including the obstacles (e.g., mountains, hills, buildings, trees, etc.) and the atmospheric conditions (e.g., precipitation, gases, etc.). Therefore, the radio signal may experience different physical phenomena during propagation, e.g., reflections, diffraction, and scattering. As a result, these factors will attenuate the received signal. The pathloss is the amount of attenuation the radio signal undergoes between the two ends of the communication link. Therefore, for efficient design and planning of any communication system, accurate RF propagation models are required to accurately predict the received signal.

Assuming that BS-A transmits a radio signal to BS-B that is separated by distance d, the received signal strength (RSS) in (dBm) at the receiving antenna of BS-B can be expressed as [20],

$$P_r(d) = P_t + G_A - L_{CA} + G_B - L_{CB} - L(d) \tag{1}$$

where P_t is the transmitted power in (dBm), (G_A and G_B) are the gain of the transmitting and receiving antennas in (dBi) respectively, (L_{CA} and L_{CB}) are the feeder cable loss (e.g., connector and cables losses) at transmitter and receiver in (dB) respectively, and $L(d)$ is the total propagation pathloss in (dB).

Most of the available propagation models are suitable for mobile communication in urban environments with little focus on rural areas. In this work, we considered the existence of a single blocking terrain in the propagation path with a small diffraction angle θ<3^o as recommended in [9]. Under this condition, reliable and cost-effective PtP NLOS backhaul links in rural areas can be guaranteed.

The proposed communication system in this work operates at Sub-6 GHz frequency (i.e., $f_c < 6$ GHz), therefore the atmospheric conditions (e.g., precipitation) can be neglected [2]. Moreover, multipath fading is unlikely to occur in rural areas taking into account the absence of the LOS path and highly directional antennas are used [5]. Thus, the total pathloss $L(d)$ in (dB) can be expressed as

$$L(d) = L_{fs}(d) + L_d(d) \tag{2}$$

where $L_{fs}(d)$ is the free space loss in (dB) and $L_d(d)$ is the diffraction loss in (dB). Therefore, the excess loss (i.e., the diffraction loss) can be obtained by subtracting the free-space loss from the total pathloss.

The free space loss in (dB) can be written as

$$L_{fs} = 32.5 + 20\log_{10}(f) + 20\log_{10}(d) \tag{3}$$

where f is the operating frequency in (MHz) and d is the distance between the transmitter and the receiver in (km).

B. RADIO PROPAGATION MODELS

In this subsection, we describe some available terrain-based radio propagation models that are suitable for modelling the pathloss and predicting the received signal strength in rural areas. The electromagnetic wave propagation models are divided into three main types: the first type is the empirical models that are based on extensive RF measurements and simple mathematical equations, but their accuracy is low. The second type is the semi-deterministic (or semi-empirical) models that are based on both RF measurement and electromagnetic theory which are more accurate than empirical models. The third type is the deterministic models which are based on the electromagnetic theory and theoretical physics such as diffraction and Fresnel theories. The semi-deterministic and deterministic models require geometrical data for the terrain profile of the propagation path. Some global DEM data sources are freely available today with high accuracy such as SRTM 1 arc-second [17]. The most used deterministic and semi-deterministic propagation models are the Longley-Rice model, aka., irregular terrain model (ITM) [21], and single/multiple knife-edge diffraction models [14], including their modified versions. These terrain-based radio propagation models have been implemented and used in most commercial and freeware radio propagation computer programs such as Radio Mobile [12], Pathloss [13], and SoftWright's terrain analysis package (TAP^{TM}) software [22].

C. IRREGULAR TERRAIN MODEL (ITM)

We will not go into details about the structure of the ITM model in this subsection as it is complex and beyond the scope of this paper but more details can be found in [23]. However, we will explain the modifications to the classic ITM model that have been implemented in some radio propagation computer software to remove the confusion regarding the different obtained diffraction loss results. The ITM model was implemented based on the electromagnetic theory and the statistical analyses of both terrain and radio measurements. The ITM model can predict the median loss

of the radio signal as a function of the distance and the variability of the signal in time and space. The ITM model was originally built using Fortran programming language as a simplification of Technical Note 101 [24]. Currently, the original ITM algorithm (version 1.2.2) is implemented in the C++ by National Telecommunications and Information Administration (NTIA) [25]. Also, the classic ITM model (v 1.2.2) is currently implemented in MATLAB and some commercial RF software such as SoftWright's TAP^{TM}. However, Radio Mobile software (v 10.0.1 and later) does not use the LOS mode of the ITM model and instead uses the classic 2-Ray model [12].

D. KNIFE-EDGE DIFFRACTION MODEL

We present a detailed description of the knife-edge diffraction model in this subsection because it is part of the rounded obstacle diffraction model adopted in this work as will be described in the next subsection. The rounded obstacle diffraction model provides the most accurate pathloss prediction results for the proposed system as discussed in Section IV. The single knife-edge model is an ideal model which approximates the blocking obstacle as a knife-edge of negligible thickness [14]. In this model, we consider any terrain that intersects with 60% of the first Fresnel zone (F1) as a blocking obstacle. The diffraction loss (i.e., Fresnel- Kirchhoff loss) using this model can be expressed as follows [14].

$$L_{ke}(v) = -10\ \log_{10}\left(\frac{[1-C(v)-S(v)]^2}{4} + \frac{[C(v)-S(v)]^2}{4}\right) \tag{4}$$

where $C(v)$ and $S(v)$ are the real and imaginary parts of the following complex Fresnel integral, respectively.

$$F(v) = \int_0^v exp\left(\frac{j\pi s^2}{2}\right)ds \tag{5}$$

The dimensionless parameter v combines all geometric parameters, see Figs. 3-4. It can be expressed in different equivalent forms as follows.

$$v = h\sqrt{\frac{2}{\lambda}\frac{d_1+d_2}{d_1 d_2}} \tag{6a}$$

$$v = \theta\sqrt{\frac{2}{\lambda}\frac{d_1 d_2}{d_1+d_2}} \tag{6b}$$

$$v = \sqrt{\frac{2h\theta}{\lambda}} \tag{6c}$$

$$v = \sqrt{\frac{2d}{\lambda}\alpha_1\alpha_2} \tag{6d}$$

where h is the distance from the top of the obstacle to the LOS line that connects the two antennas (h is negative if the obstacle is below this line), (d_1, d_2) are the distances from the antennas to the top of the obstacle, d is the path length, θ is the angle of diffraction, and (α_1, α_2) are the angles between the line that connects the top of the obstacle to the antennas and the LOS line. The angles (θ, α_1, and α_2) have the same signs as that of h and have a unit of radians (rad). The parameters (h, d, d_1, d_2, and λ) must have self-consistent units, e.g., meter.

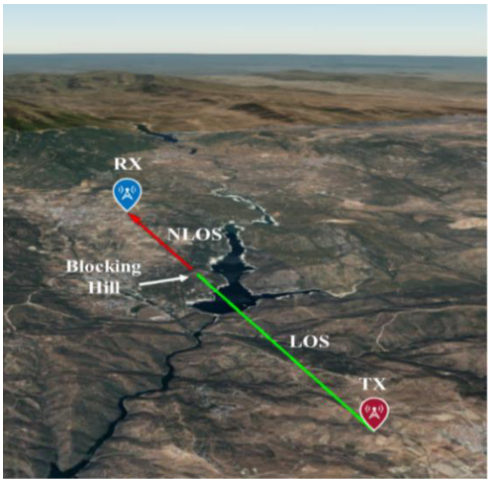

FIGURE 3. Satellite image of one of the sites under analysis (i.e., site index 1) using SRTM 1 arc-second global DEM.

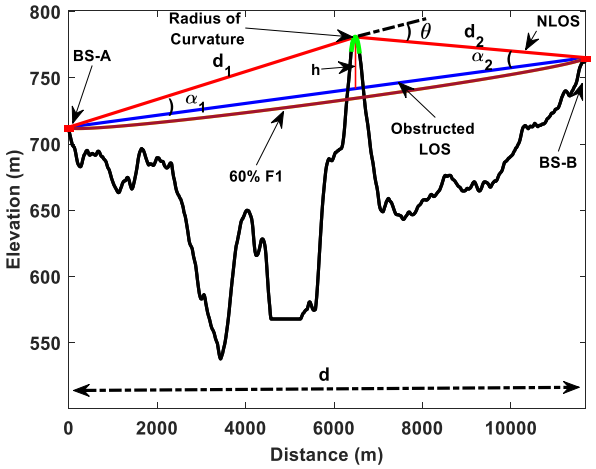

FIGURE 4. Path elevation profile and geometric parameters based on SRTM 1 arc-second global DEM for site.

E. ROUNDED OBSTACLE DIFFRACTION MODEL

In this subsection, we will introduce an improved diffraction model based on the knife-edge diffraction model considering the radius of curvature at the obstacle top (i.e., rounded obstacle diffraction model). The real obstacles have a thickness which can be approximated as a thick rounded obstacle with a radius of curvature (R) at the top. Therefore, the additional attenuation due to the curvature of the obstacle can be added to Fresnel- Kirchhoff loss in Eq. (4) to get the total diffraction loss as follows [14].

$$L_d = L_{\text{ke}}(v) + T(m,n) \tag{7}$$

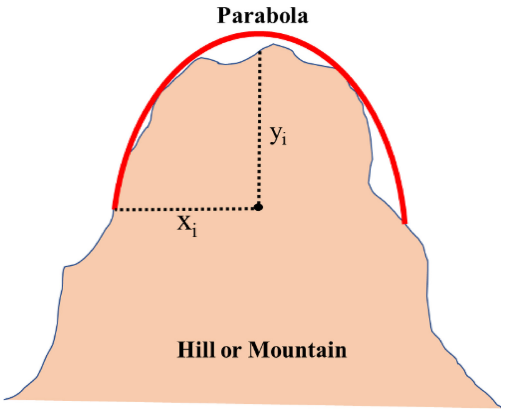

FIGURE 5. Vertical profile of the obstacle with a parabola fit to the top of the obstacle.

where $T(m, n)$ is given in (dB) as follows:

$$T(m,n) = M(m,n) - \ (22.5n)m, \ \ mn \leq 4 \tag{8a}$$

$$T(m,n) = M(m,n) - 6 - 20\log_{10}(\text{mn}) - \ (2 - 17n)m, \ \ mn > 4 \tag{8b}$$

The factor $M(m, n)$ is expressed as

$$M(m,n) = 7.2m^{\frac{1}{2}} + 3.6m^{\frac{3}{2}} + 7.2m^{\frac{1}{2}} - 0.8m^2 \tag{9}$$

where n and m parameters are given as

$$m = \frac{R(d_1 + d_2)}{d_1 d_2 U^{1/3}} \tag{10}$$

$$n = \frac{hU^{2/3}}{R} \tag{11}$$

$$U = \frac{\pi \mathrm{R}}{\lambda} \tag{12}$$

The obstacle radius of curvature corresponds to the radius of curvature at the apex of a parabola fitted to the obstacle profile in the vicinity of the top as shown in Fig. 5. In this calculation, the maximum vertical distance from the apex should be of the order of first Fresnel zone radius (F1) where the obstacle is located. Thus, the mean radius of the curvature of the obstacle is given as

$$R = \frac{1}{N}\sum_{1}^{N}\frac{x_i^2}{2\ y_i} \tag{13}$$

where x_i and y_i are the horizontal and vertical distances for the i-th sample and N is the total number of samples.

In this work, the predicted diffraction loss using different terrain-based propagation models is compared with the measured data for five rural sites as given in [9, Table 2]. The obtained geometric parameters using the rounded-obstacle diffraction model for these sites are given in Table 1 below. The predicted diffraction loss is obtained using the single knife-edge model, the rounded-obstacle diffraction model, the classic ITM model, and the modified ITM model in Radio Mobile software. We evaluate these models based on SRTM 1 arc-second global DEM. Also, the predicted results

TABLE 1. The obtained geometric parameters in the rounded-obstacle diffraction model.

Site Index	h_A (m)	h_B (m)	d_1 (km)	d_2 (km)	d (km)	h (m)	F1 (m)	R (m)
1	2	2	6.47	5.21	11.68	39	12	421
2	2	2	9.00	12.01	21.02	99	16	688
3	2	2	14.56	26.04	40.60	28	22	325
4	2	2	14.00	25.60	39.60	106	22	336
5	35	2	44.35	19.93	64.28	135	27	262

TABLE 2. Cambium PTP550E transmit power in (dBm).

MCS			Channel BW (MHz)		
MCS	**Modulation**	**Coding Rate**	**20**	**40**	**80**
MCS1	QPSK	1/2	25	23	23
MCS2	QPSK	3/4	25	23	23
MCS3	16-QAM	1/2	25	23	23
MCS4	16-QAM	3/4	23	23	23
MCS5	64-QAM	2/3	22	22	22
MCS6	64-QAM	3/4	21	21	21
MCS7	64-QAM	5/6	20	20	20
MCS8	256-QAM	3/4	20	20	20
MCS9	256-QAM	5/6	19	19	19

are compared with the obtained diffraction loss using the ITM and TIREM™ models in Pathloss 5.0 software as given in [9, Table 2].

III. END-TO-END NLOS WIRELESS BACKHAUL SYSTEM

In the previous section, we present the radio propagation models used to predict the pathloss that arises in the NLOS propagation channel in rural areas at 5.8 GHz frequency. In this section, we will describe the end-to-end wireless communication system used to evaluate the performance and feasibility of the PtP NLOS backhaul in terms of packet error rate (PER) and throughput.

A. STRUCTURE AND COMPONENTS OF THE END-TO-END NLOS WIRELESS BACKHAUL SYSTEM

In this subsection, we present the proposed NLOS wireless backhaul system based on the IEEE 802.11ac standard including transmitter, receiver, and channel as shown in Fig. 6. User data are randomly generated and fed into a forward error correction (FEC) encoder that can use either binary convolutional code (BCC) or low-density parity-check code (LDPC). In this system, we use BCC with different coding rates. Then, the coded data are modulated using different modulation schemes, i.e., QPSK to 256-QAM. The supported channel bandwidths (BWs) in this system are 20 MHz, 40 MHz, and 80 MHz. The modulated signal is amplified and transmitted via the antenna into the channel. The transmitted signal is attenuated by the pathloss, which is predicated using the rounded-obstacle diffraction model

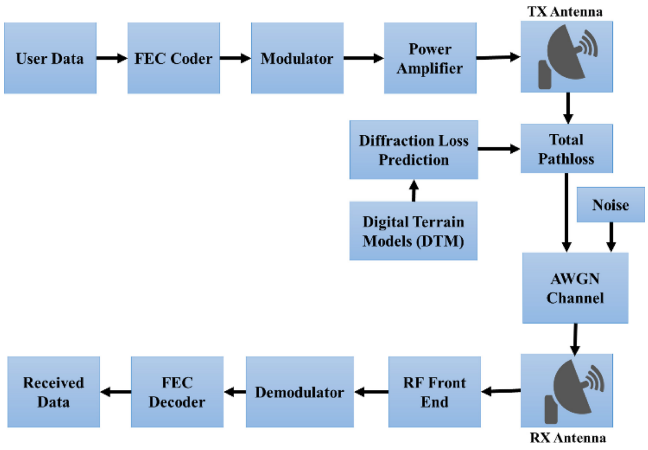

FIGURE 6. Simplified illustration of end-to-end NLOS wireless backhaul system.

described in Section II. Also, the received signal is corrupted by thermal noise in the RF front-end of the receiver which is modelled as an additive white Gaussian noise (AWGN). Then the received signal is demodulated and decoded using a Viterbi decoder to reconstruct the transmitted data, i.e., the PLCP service data unit (PSDU). The PER is calculated by comparing the recovered packets (i.e., PSDUs) with the transmitted packets to find the number of error packets. A received packet is incorrect if at least one bit in the packet is erroneous. Throughput measures the number of packets successfully received per unit of time. Thus, the PER and throughput in (Mbps) can be calculated as follows.

$$PER = \frac{Num\ Packet\ Errors}{Total\ Transmit\ Packets} \tag{14}$$

$$Throughput = \frac{m(1 - PER)}{T_p \times 10^6} \tag{15}$$

where m is the packet length in bits and T_p is the packet duration in seconds.

B. IEEE 802.11AC (WI-FI 5) STANDARD-BASED RADIO TRANSCEIVERS

In this subsection, we briefly present the IEEE WLAN standards and commercial radio equipment operating in the Sub-6 GHz band. Today, many commercial PtP wireless backhaul solutions are available in the market that operate in the Sub-6 GHz band based on the 5th and 6th generation of WLAN standards, i.e., Wi-Fi 5 (IEEE 802.11ac) and Wi-Fi 6 (IEEE 802.11ax) [26]. This technology is a low-cost option that is easy to install and provides adequate capacity to support broadband services. The IEEE 802.11ac is an emerging WLAN standard developed by the IEEE 802.11ac task group (TGac) that provides very high throughput (VHT) and signal bandwidth of up to 160 MHz. In addition, a new Wi-Fi 7 (IEEE 802.11be) is an upcoming standard that operates at (2.4 GHz, 5 GHz, and 6 GHz) and will support extremely high throughput (EHT). To make the simulation and modelling more realistic, the radio transceivers on both BSs are considered to have specifications similar to the commercial PTP550E radio equipment manufactured by Cambium Networks [26]. Cambium PTP550E is an outdoor PtP radio device based on the IEEE 802.11ac standard that includes both radio and networking electronics as a wireless Ethernet bridge solution. It operates in the frequency band of 4.9-6.2 GHz and supports various MCS, e.g., MCS0-MCS9, with a maximum throughput of up to 1.4 Gbps (when operating with 160 MHz aggregated channel BW). Cambium PTP550E is available as an integrated unit with a 23 dBi antenna or as a connectorized unit with an external antenna. In our work, we have assumed that the same radio unit is used at both ends of the link with an external directional parabolic antenna to increase the system range and gain within the maximum permissible effective isotropic radiated power (EIRP). According to FCC rules for unlicensed PtP fixed wireless equipment (e.g., high-speed and high-capacity Wi-Fi) operating in the ISM band (5.725-5.875 GHz), the maximum allowable EIRP is 53 dBm [27]. According to the FCC, several telecommunications companies and wireless Internet service providers (WISPs) oppose the proposal to limit the EIRP for PtP fixed wireless systems. For example, Cambium believes that the new rules will make it more difficult to deploy long-range wireless backhauls in rural and hard-to-reach areas [27]. Moreover, while the cost-effective NLOS systems can operate in an unlicensed band, the licensed band link would require one or more repeaters. Following these rules, we show that a feasible NLOS backhaul link can still be achieved at a distance of 11 km in rural areas. The maximum transmit power from Cambium PTP550E for various MCS at different channel BWs is listed in Table 2. The EIRP in (dBm) can be expressed as

$$EIRP = P_t + G_A - L_{CA} \tag{16}$$

In the experimental setup of the PtP NLOS backhauls, the antennas should be carefully aligned toward the top of the obstacle in azimuth and elevation directions to get the highest received signal. The antenna alignment can be performed mechanically or through automated beamforming techniques. However, it is found that mechanical antenna alignment is relatively easy in the practical measurement setup [2], [28].

C. THERMAL NOISE POWER AND NOISE FIGURE OF THE RF FRONT END

The approach used to estimate the signal-to-noise ratio (SNR) at the receiver is introduced in this subsection. The SNR is obtained based on the calculated thermal noise power and the estimated received signal using realistic characteristics of the radio transceiver such as sensitivity and maximum transmitted power. The performance of the PtP NLOS backhaul is quantified by the PER and achieved throughput in the presence of thermal noise and propagation pathloss. As we mentioned before, another impairment that affects the performance of the digital communication system is thermal noise at the RF front end of the receiver, see Fig. 7. Each electronic component contributes a minimum amount of noise proportional to the temperature. Thermal noise is the

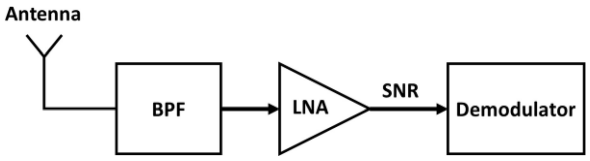

FIGURE 7. Simplified illustration of a receiver RF front-end (demodulator is not included).

main noise source that is always presented and added to the received signal at the input of the receiver. The noise is flat, i.e., it has uniform power spectral density (PSD), over the entire frequency spectrum and its amplitude can be modelled using a normal probability distribution with zero mean and variance of σ^2. Therefore, thermal noise can be modelled as an AWGN. The AWGN channel is usually used to model the PtP terrestrial wireless links and satellite communications links, assuming that the multipath fading and interference are negligible in the channel [5]. In PtP microwave links in rural areas, interference and multipath are unlikely to occur and are therefore neglected in this system, especially with the use of high-performance directional antennas [5]. The received signal is equal to the transmitted signal attenuated by the pathloss and corrupted by the additive noise as

$$r = a\ s + n \tag{17}$$

where r is the received signal at the receiver input, s is the transmitted signal, a is the attenuation factor due to pathloss, and n is the additive noise that follows the normal probability distribution $n \sim N(0, \sigma^2)$.

The estimation of SNR is essential for the efficient and accurate design of PtP wireless backhaul links which provides insight into the performance and feasibility of the deployed systems. Therefore, we need to find the SNR which is the main input parameter for the AWGN channel in the simulation framework. The SNR at the receiver is determined as a ratio of the average signal power after attenuation to the noise power. The SNR at the receiver is defined in (dB) as

$$SNR = P_r - P_n \tag{18}$$

where P_n is the average noise power (i.e., noise floor) in (dBm).

The noise from each component in the receiver's front end is added to the receiver's noise floor. The noise floor has a direct impact on the minimum received signal level that can be detected and demodulated, i.e., the receiver sensitivity. We assume the filter has a unity gain and causes a negligible attenuation to the signal power.

Noise is characterized by its PSD, i.e., N_0, which is the power in a 1 Hz BW and is given in (W/Hz) units. Nyquist showed that the noise PSD can be expressed as

$$\frac{N_0}{2} = k_B T \tag{19}$$

where $k_B = 1.380649 \times 10^{-23}$ is the Boltzmann constant in (J/K) and T is the absolute temperature in Kelvin at the receiver front-end. The minimum equivalent input noise for the receiver at room temperature (290 K) is $N_0 = -174$ dBm/Hz.

TABLE 3. Cambium PTP550E receiver sensitivity in (dBm).

MCS			Channel BW (MHz)		
MCS	**Modulation**	**Coding Rate**	**20**	**40**	**80**
MCS1	QPSK	1/2	-88	-85	-83
MCS2	QPSK	3/4	-86	-83	-81
MCS3	16-QAM	1/2	-83	-81	-79
MCS4	16-QAM	3/4	-81	-79	-77
MCS5	64-QAM	2/3	-77	-74	-72
MCS6	64-QAM	3/4	-75	-73	-71
MCS7	64-QAM	5/6	-73	-71	-69
MCS8	256-QAM	3/4	-69	-67	-65
MCS9	256-QAM	5/6	-67	-65	-63

The noise power at the output of the receiving filter in (dBm) is equal to [29]:

$$P_n = -174 + \mathrm{NF} + 10\log_{10}(BW_{eq}) \tag{20}$$

where NF is the noise figure of the receiver in (dB) and BW_{eq} is the equivalent noise BW of the receiver. It is worth mentioning that the low-noise amplifier (LNA) represents the dominant contribution to the NF. Nowadays, many RF front-end modules (FEMs) are manufactured with high performance that supports the WLAN standards such as Wi-Fi 5 and Wi-Fi 6 [30], [31], [32], [33]. These modules consist of high-performance LNAs and filters with a low NF of less than 3 dB.

In digital communication systems, receiver sensitivity refers to the minimum received signal power for a receiver to accurately demodulate the signal. The receiver sensitivity is a function of the band-limited thermal noise, receiver noise figure (NF), and minimum SNR ($\mathrm{SNR_{min}}$) required for a particular modulation to accurately demodulate the symbols. The sensitivity can be expressed in (dBm) as

$$P_s = P_n + SNR_{min} \tag{21}$$

The $\mathrm{SNR_{min}}$ and consequently the receiver sensitivity is usually defined at a specific BER or PER. For IEEE 802.11ac, successful demodulation is determined by a PER less than 10% for a PSDU length of 4096 octets [34], [35]. A smaller sensitivity value indicates better receiver performance. The receiver sensitivity depends on the BW, the modulation scheme, and the coding rate. In our model, we use the sensitivity table of the Cambium PTP550E radio unit as listed in Table 3, extracted from the product datasheet [26]. The performance of the PtP NLOS wireless backhaul system described here will be evaluated in the next section.

IV. RESULTS

In this section, we first show the diffraction loss prediction results and the corresponding accuracy compared to the measured data for PtP NLOS links in an unlicensed 5.8 GHz band in five rural sites located in Spain as given in [9, Table 2]. The predicted diffraction loss and free space loss represent the large-scale fading impermeant in the

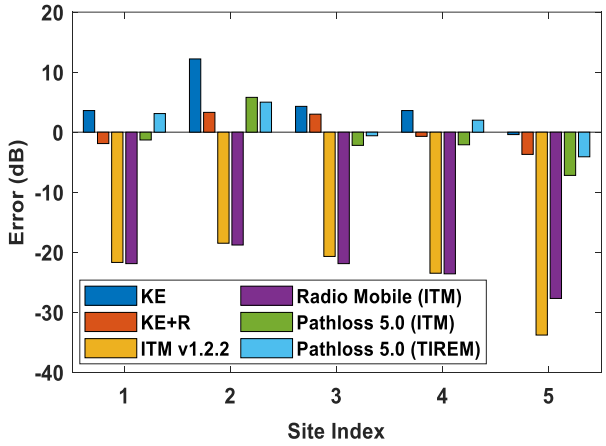

FIGURE 8. The error between measured and predicted diffraction loss using various RF propagation models.

TABLE 4. Predicted and measured diffraction loss using various propagation models and software.

Model \ Site Index	Diffraction Loss (dB) 1	2	3	4	5	Avg. Error (dB)	RMSE (dB)
Knife-Edge (KE)	26.0	31.8	18.3	29.8	30.1	4.7	6.2
KE with Radius (KE+R)	31.5	40.7	19.6	34.1	33.4	**-0.01**	**2.7**
MATLAB (ITM v1.2.2)	51.3	62.5	43.3	56.9	63.5	-23.6	24.2
Radio Mobile (ITM)	51.5	62.8	44.5	57	57.4	-22.8	23.0
Pathloss 5.0 (ITM)	30.9	38.2	24.8	35.5	36.9	-1.4	4.4
Pathloss 5.0 (TIREM)	26.5	39.0	23.2	31.4	33.8	1.1	3.3
Measured loss	29.6	44	22.6	33.4	29.7	-	-

channel. The accuracy of diffraction loss prediction is evaluated using different RF propagation models including the classic ITM model (v1.2.2), the modified ITM versions in Radio Mobile and Pathloss 5.0, the rounded-obstacle diffraction model, and the TIREM model. The geographical coordinates and antenna heights of BS-A and BS-B with the corresponding measured diffraction loss at these sites are given in [9, Table 2]. The NLOS radio propagation path in these rural sites has a single dominant blocking terrain with a small diffraction angle, i.e., θ<3°. For a fair comparison, we use global SRTM 1 arc-second (30m resolution) DEM as the primary elevation data source for all propagation models under analysis. We predict the pathloss for different antenna heights at both base stations (BSs). Then, we evaluate the performance of an end-to-end wireless NLOS communication system via simulation using IEEE 802.11ac wireless technology at one of these rural sites.

As shown in Table 4 and Fig. 8, we present the predicted diffraction loss and prediction error using different RF propagation models compared to the measured data. As mentioned in Section II, some RF design software have made some modifications to the classic ITM model (v1.2.2). Therefore, the ITM model implemented in different RF design software may give different pathloss prediction results. We obtained the predicted loss using the ITM model in Radio Mobile software and the classic ITM (v1.2.2) in MATLAB. Furthermore, we present the diffraction loss obtained in Pathloss 5.0 software based on the ITM and the TIREM models from [9, Table 2]. Both the Pathloss 5.0 software and the TIREM model are commercial software that requires a license. Finally, we implement an algorithm in MATLAB to calculate the diffraction loss using both the knife-edge (KE) model and the rounded-obstacle diffraction model, i.e., the KE model with the obstacle radius of curvature (KE+R). The obtained geometric parameters in the rounded-obstacle diffraction model for these sites are listed in Table 1.

We can observe that the classic ITM (v1.2.2) and the ITM in Radio Mobile software largely overestimate the diffraction loss with an average error of (−23.6, −22.8) dB and RMSE values of (24.2, 23) dB, respectively. Here, negative error values mean that the predicted loss is larger than the measured loss. However, the ITM and TIREM models in Pathloss 5.0 software slightly overestimate/underestimate the diffraction loss with an average error of (−1.4, 1.1) dB and RMSE values of (4.4, 3.3) dB, respectively. The rounded-obstacle diffraction model provides the best prediction accuracy compared to other models with a negligible average error of −0.01 dB and RMSE value of 2.7 dB while the KE model underestimates the diffraction loss with an average error of 4.7 dB and RMSE of 6.2 dB. Therefore, the rounded-obstacle diffraction model will be adopted to model the large-scale fading in the communication channel to evaluate the end-to-end performance analysis of the PtP NLOS wireless backhaul. Thus, the rounded-obstacle diffraction model in such a scenario provides satisfactory results as a cost-effective option compared to commercial RF software which may cost thousands of dollars.

We will now evaluate the performance of the end-to-end NLOS wireless link between BS-A and BS-B at the rural site of an index (1) that has geographic coordinates listed in Table 5. The parameters used in the RF propagation models and link budget calculation are listed in Table 5. We evaluate the performance in terms of PER, throughput, and fade margin (FM) for a range of antenna heights (i.e., 5-20 m) at both BSs. To make the model more realistic, the maximum transmitted power and sensitivity of the transmitting and receiving BSs are chosen based on the RF characteristic of the Cambium PTP550E unit for various MCSs and channel BWs as listed in Tables 2 and 3. The Cambium PTP550E is a 5 GHz PtP microwave radio unit based on the IEEE 802.11ac (Wi-Fi 5) standard. The antenna gain is chosen such that the regulatory limit of the EIRP with this radio unit is not exceeded. The NF value of the receiver was chosen to reflect the typical value in this frequency band.

TABLE 5. RF link budget and pathloss model parameters.

Parameter	Value	Unit	Description
f_c	5800	MHz	Carrier frequency.
d	11.6	Km	Distance between BS-A and BS-B
h_A	5-20	m	Antenna height of BS-A above ground level.
h_B	5-20	m	Antenna height of BS-B above ground level.
P_t	19 – 25	dBm	Transmit power.
G_A, G_B	31	dBi	Antenna gain of BS-A and BS-B.
L_{CA}, L_{CB}	1	dB	Feeder cable loss of BS-A and BS-B.
P_s	-88 to -63	dBm	Receiver sensitivity.
NF	3	dB	Receiver noise figure.
$(lat, lon)_A$	40.375111 -4.258472	deg.	Latitude and longitude of BS-A in the site of index 1.
$(lat, lon)_B$	40.375833 -4.396055	deg.	Latitude and longitude of BS-B in the site of index 1.

TABLE 6. Predicted link budget parameters for various antenna heights using MCS3 and MCS4 at 80 MHz channel BW.

Antenna Height Index (h_{index})	h_A (m)	h_B (m)	L_d (dB)	θ deg.	P_r (dBm)	SNR (dB)
1	5	5	30.44	0.71	-76.56	16.35
2	5	10	29.39	0.66	-75.51	17.40
3	5	15	28.28	0.60	-74.40	18.51
4	5	20	27.11	0.55	-73.23	19.68
5	10	5	29.60	0.67	-75.72	17.19
6	10	10	28.51	0.61	-74.63	18.28
7	10	15	27.34	0.56	-73.46	19.45
8	10	20	26.10	0.50	-72.22	20.69
9	15	5	28.73	0.62	-74.85	18.06
10	15	10	27.58	0.57	-73.70	19.21
11	15	15	26.35	0.51	-72.47	20.44
12	15	20	25.03	0.46	-71.15	21.76
13	20	5	27.81	0.58	-73.93	18.98
14	20	10	26.60	0.53	-72.72	20.19
15	20	15	25.30	0.47	-71.42	21.49
16	20	20	23.89	0.42	-70.01	22.90
Min			23.89	0.42	-76.56	16.35
Max			30.44	0.71	-70.01	22.90
Avg.			27.38	0.56	-73.50	19.41

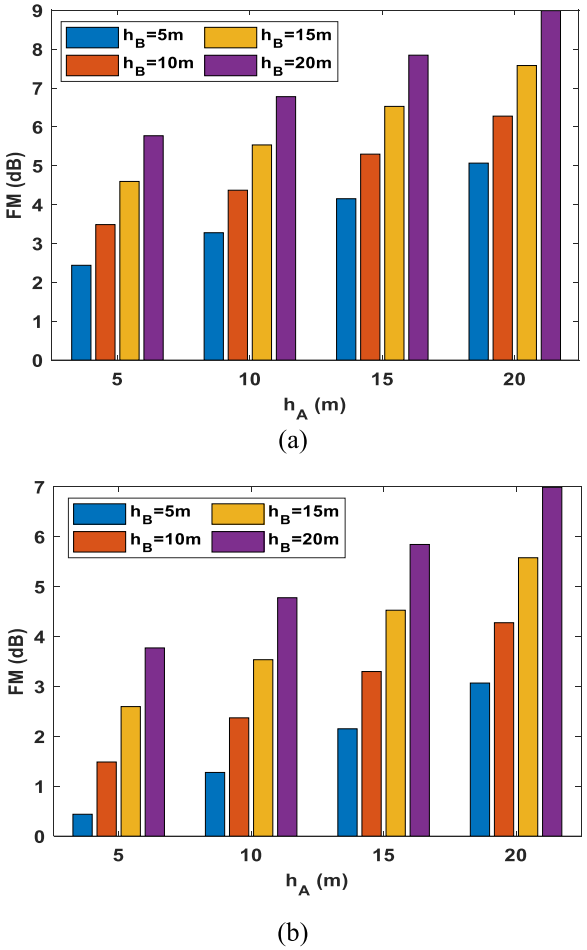

FIGURE 9. Fade margin (FM) for various antenna heights of BS-A and BS-B at 80 MHz channel BW using (a) MCS3 and (b) MCS4.

The predicted link budget parameters are listed in Table 6 based on the rounded-obstacle diffraction model for different antenna heights of BS-A (h_A) and BS-B (h_B). As will be demonstrated later, we find that the NLOS backhaul links with reliable performance for various antenna heights can be mainly achieved using MCS3 and MCS4 for the channel BW of 80 MHz. Therefore, in Table 6 and Fig. 9, we present only the predicted data for MCS3 and MCS4 at 80 MHz channel BW. The received signal strength (P_r) and the SNR are calculated using Eqs. (1)–(3) and Eqs. (18)–(20), respectively. The fade margin (FM) shown in Fig. 9 is calculated by subtracting the receiver sensitivity (P_s) from the received signal strength (P_r). In fact, the large FM needed for conventional LOS microwave links over long distances is not required here for NLOS links over short distances, e.g., 10-20 km. The results show that increasing the height of the BS-A or BS-B antenna leads to an increase in the received signal strength, and consequently the SNR and FM. This occurs due to a decrease in the diffraction angle (θ) which leads to a reduction in the diffraction loss (L_d). Increasing the antenna height of BS-A or BS-B from 5m to 20m will reduce diffraction loss and thus improve SNR and FM by 3.25 dB on average. The antenna height configuration (index 16) can reduce the diffraction loss and consequently improve SNR and FM by 6.5 dB on average compared to the antenna height configuration (index 1). It is worth mentioning that increasing the antenna height will increase the deployment cost of the tower including the cost of materials. Therefore, it is necessary to choose suitable tower heights that satisfy the performance requirements at the lowest cost in such rural areas.

The performance of the proposed system is evaluated in terms of achieved throughput and PER via an end-to-end simulation of the IEEE 802.11ac^{TM} wireless link in MATLAB for different MCSs and channel BWs. In this system, the thermal noise is modelled as an AWGN in the communication channel. The predicted pathloss and noise power are used to calculate the SNR which is a primary input for the AWGN channel. For each SNR value, many packets (N_p=10^4) are transmitted through the channel and then demodulated and decoded at the receiver. The recovered packets (i.e., PSDUs) are compared with the

TABLE 7. System parameters for the IEEE 802.11ac end-to-end wireless link simulation.

Parameter	Value	Unit	Description
MCS	1-9	-	Modulation and coding scheme.
GI	800 (long)	ns	Guard interval.
PSDU length	4096	bytes	Packet length.
FEC	BCC	-	Forward error correction using binary convolutional coding.
STBC	Disabled	-	Space-time block coding.
BW	20, 40, 80	MHz	Channel BW.
N_p	10^4	-	Maximum number of transmitted packets.
N_E	10^3		Maximum number of packet errors.
n_{tx}	1	-	Number of transmit antennas.
n_{rx}	1	-	Number of receive antennas.
n_s	1	-	Number of space-time streams.

transmitted packets to calculate the number of packet errors and thus the PER and throughput using Eqs. (14) and (15). The PER and throughput assess the end-to-end system performance including the transmitter, the receiver, and the channel. The simulation is controlled using two parameters that determine the duration of the simulation, namely, the maximum number of packet errors (N_E) and the maximum number of transmitted packets (N_P). When either the number of packet errors or the number of transmitted packets reaches, the simulation will stop. The simulation parameters for the IEEE 802.11ac™ wireless link are listed in Table 7.

The PER and throughput are plotted for a range of SNR values in Figs. 10 and 11, respectively. In general, a higher MCS index leads to higher spectral efficiency and thus higher throughput as shown in Fig. 11. For example, the maximum throughput that can be achieved using 80 MHz channel BW is 100 Mbps for MCS3 and 143 Mbps for MCS4. However, as the MCS index increases, we should expect a larger PER, as the demodulation process becomes harder in the receiver, see Fig. 10. For instance, the PER for SNR=15 dB is almost zero for MCS3 and one for MCS4. A higher MCS index requires a larger SNR at the receiver to correctly demodulate the signal because the separation distance between the constellation points becomes smaller. For example, we can observe that a minimum SNR of about 15 dB and 18 dB is required to accurately recover the transmitted packets with a throughput of 100 Mbps and 143 Mbps, using MCS 3 and MCS 4 at 80 MHz channel BW, respectively. Moreover, a larger channel BW will allow a higher data rate to be transferred as shown in Fig. 11, but this will increase noise and reduce the SNR at the receiver. For instance, the maximum achieved throughput using MCS4 is 37 Mbps, 73 Mbps, and 143 Mbps for channel BW of 20 MHz, 40 MHz, and 80 MHz, respectively.

In this work, we mainly focus on evaluating the feasibility of PtP NLOS backhaul links via diffraction in rural areas. In rural and remote areas with a low population density, the required throughput is not as high as in urban regions for a good user quality of experience (QoE). Usually, people in rural areas need access to the Internet to connect with friends

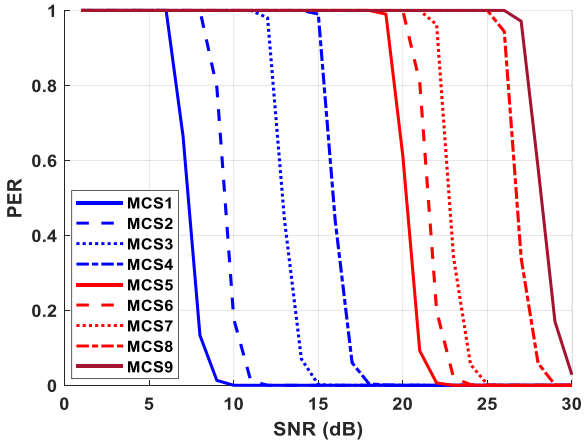

FIGURE 10. PER versus SNR for different MCSs at 80 MHz channel BW.

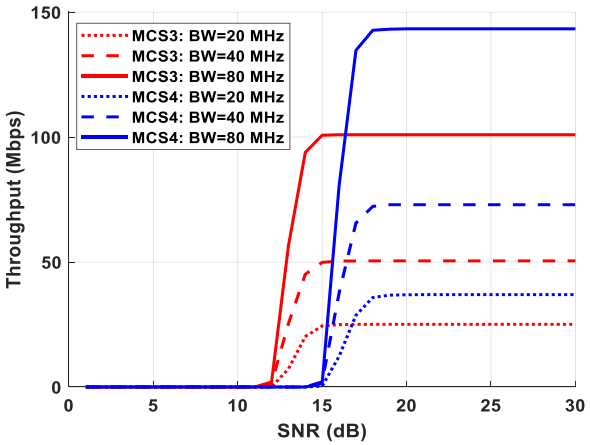

FIGURE 11. Throughput versus SNR for MCS3 and MCS4 at different channel BWs.

and family, work remotely, stay up-to-date with current events, access different online services such as educational and economic platforms, etc. Therefore a throughput of 100-150 Mbps is sufficient for such needs in sparsely populated rural areas [36], [37]. This is comparable to the throughput offered using satellite backhauls in rural areas and the throughput of small LTE cells in urban areas [38]. Moreover, the maximum acceptable PER is set to 10% which is required to successfully demodulate the received signal in IEEE 802.11ac-based systems [34], [35]. Therefore, in this work, we assume a feasible wireless backhaul link can be guaranteed for a throughput larger than 100 Mbps and a PER of less than 10%.

Figure 12 shows the achieved throughput with the corresponding PER using MCS3-MCS6 for various antenna heights. Results for other MCS indices are not shown here because they do not provide the required throughput or the acceptable PER. The results in this figure are plotted for 80 MHz channel BW except for MCS6 which is plotted for 40 MHz BW. Using MCS3, a throughput of up to 100 Mbps can be achieved with a PER<1% for all antenna height configurations. We can see that MCS4 does not satisfy the required performance (i.e., PER>10%) for

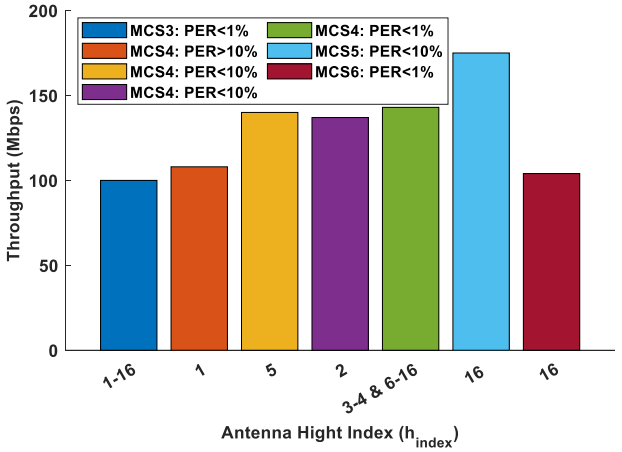

FIGURE 12. Achieved throughput with corresponding PER at various antenna heights for MCS3-MCS5 at 80 MHz BW and MCS6 at 40 MHz BW.

h_{index}=1. However, using MCS4 can provide up to 140 Mbps throughput with PER<10% for h_{index}= {2, 5} and PER<1% for h_{index}= {3-4, 6-16}. A higher data rate (i.e., 175 Mbps) with PER<10% can be obtained using MCS5 but only when the antenna height configuration is chosen as h_{index}=16 (i.e., $h_A = h_b = 20$m). This is because a higher MCS index requires a larger SNR to accurately demodulate the received signal which is achieved here by increasing the antenna height. Finally, MCS6 provides a data rate of about 100 Mbps with PER<1% using 40 MHz channel BW. In general, the results show that a throughput of 100-175 Mbps with PER<10% can be achieved for an NLOS backhaul link at a distance of 11 km in a rural area using MCS3-MCS6 and channel BW of 40-80 MHz. These results can provide useful guidance for choosing optimal design parameters to achieve wireless backhaul links in rural areas with the required performance.

V. CONCLUSION

In this work, we examine the feasibility of PtP NLOS wireless backhaul link via diffraction in an unlicensed 5.8 GHz band in rural areas. Accurate modelling of the diffraction in this scenario plays an important role in calculating the link budget and choosing optimal system parameters to obtain viable NLOS wireless links. Therefore, we evaluate the accuracy of different terrain-based propagation models in predicting diffraction compared to measured data for different antenna heights. The classic ITM model and its modified version in Radio Mobile software significantly overestimate the diffraction loss. For example, the classic ITM (v1.2.2) and the ITM in Radio Mobile software largely overestimate the diffraction loss with an average error of (−23.6, −22.8) dB and RMSE values of (24.2, 23) dB, respectively. However, the rounded-obstacle diffraction model gives the best prediction accuracy with a negligible average error and an RMSE value of 2.7 dB. The performance and feasibility of the proposed system are evaluated in terms of PER and throughput via an end-to-end simulation based on IEEE 802.11ac^{TM} wireless technology. The results show that an NLOS backhaul link in rural areas is feasible over a distance of 11 km with a throughput of 100-175 Mbps and a PER between 0-10%. This performance is achieved using MCS3-MCS6, channel BW of 40-80 MHz, and antenna heights between 5-20m. This work can help in the optimum planning and design of NLOS wireless backhauls via diffraction before deployment while saving time and cost which is a critical factor in low-income rural areas. In future work, we will study the feasibility of NLOS backhaul links over higher frequencies and longer distances considering the effect of the potential interference.

REFERENCES

[1] D. Bogdan-Martin, "Measuring digital development: Facts and figures 2022," Int. Telecommun. Union (ITU), Geneva, Switzerland, 2022.
[2] M. Coldrey, J.-E. Berg, L. Manholm, C. Larsson, and J. Hansryd, "Non-line-of-sight small cell backhauling using microwave technology," *IEEE Commun. Mag.*, vol. 51, no. 9, pp. 78–84, Sep. 2013.
[3] J. Kusuma, E. Boch, and P. Liddell, *Diffractive NLOS Microwave Backhaul for Rural Connectivity*, Telecom Infra Project, Wakefield, MA, USA, 2021.
[4] Z. El Khaled, W. Ajib, and H. Mcheick, "Log distance path loss model: Application and improvement for sub 5 GHz rural fixed wireless networks," *IEEE Access*, vol. 10, pp. 52020–52029, 2022.
[5] Z. Zaidi and K.-C. Lan, "Wireless multihop backhauls for rural areas: A preliminary study," *PloS ONE*, vol. 12, no. 4, 2017, Art. no. e0175358.
[6] G. R. MacCartney Jr et al., "Millimeter wave wireless communications: New results for rural connectivity," in *Proc. 5th Workshop All Things Cell. Operat. Appl. Challenges*, 2016, pp. 31–36.
[7] G. R. MacCartney and T. S. Rappaport, "Rural macrocell path loss models for millimeter wave wireless communications," *IEEE J. Sel. Areas Commun.*, vol. 35, no. 7, pp. 1663–1677, Jul. 2017.
[8] H. Lehpamer, *Microwave Transmission Networks: Planning, Design, and Deployment*. New York, NY, USA: McGraw-Hill Educ., 2010.
[9] J. Kusuma and E. Boch, "Improving rural connectivity coverage using diffractive non-line of sight (NLOS) wireless backhaul," in *Proc. World Wireless Res. Forum*, vol. 45, 2021. [Online]. Available: https://research.fb.com/wpcontent/uploads/2021/01/Improving-RuralConnectivity-Coverage-using-Diffractive-Non-Lineof-Sight-NLOS-Wireless-Backhaul.pdf
[10] E. Boch and J. Kusuma, "Combining CLOS and NLOS microwave backhaul to help solve the rural connectivity challenge," *Microw. J.*, vol. 64, no. 5, pp. 80–88, 2021.
[11] E. J. Oughton, E. Boch, and J. Kusuma, "Engineering-economic evaluation of diffractive NLOS backhaul (e3nb): A techno-economic model for 3D wireless backhaul assessment," *IEEE Access*, vol. 10, pp. 3430–3446, 2022.
[12] VE2DBE. "Radio mobile software." 2020. Accessed: Jul. 24, 2023. [Online]. Available: https://www.ve2dbe.com/english1.html
[13] (Contract Telecommun. Eng. Ltd., Delta, BC, Canada). *Pathloss*. (2016). Accessed: Jul. 24, 2023. [Online]. Available: https://www.pathloss.com/
[14] "Propagation by diffraction," Int. Telecommun. Union (ITU), Geneva, Switzerland, ITU-Recommendation P. 526–15, 2019.
[15] D. Eppink and W. Kuebler, "TIREM/SEM handbook," Dept. Defense, Electromagn. Compatibil. Anal. Center, Annapolis, MD, USA, Rep. ECAC-HDBK-93-076, 1994.
[16] (Alion Sci. Technol. Corp., McLean, VA, USA). *The Terrain Integrated Rough Earth Model (TIREM^{TM})*. (2023). Accessed: Jul. 24, 2023. [Online]. Available: https://rfspectrummodels.alionscience.com/ModelStorefront/productTemplate?id=110
[17] (Open Topography, San Diego, CA, USA). *Shuttle Radar Topography Mission (SRTM) Global*. (2023). [Online]. Available: https://doi.org/10.5069/G9445JDF
[18] S. Kasampalis, P. I. Lazaridis, Z. D. Zaharis, A. Bizopoulos, S. Zettas, and J. Cosmas, "Comparison of ITM and ITWOM propagation models for DVB-T coverage prediction," in *Proc. IEEE Int. Symp. Broadband Multimedia Syst. Broadcast. (BMSB)*, 2013, pp. 1–4.

[19] S. Kasampalis, P. I. Lazaridis, Z. D. Zaharis, A. Bizopoulos, S. Zettas, and J. Cosmas, "Comparison of longley-rice, ITM and ITWOM propagation models for DTV and FM broadcasting," in *Proc. 16th Int. Symp. Wireless Personal Multimedia Commun. (WPMC)*, Atlantic City, NJ, USA, 2013, pp. 1–6.
[20] M. S. Al Salameh and M. M. Al-Zu'bi, "Prediction of radiowave propagation for wireless cellular networks in Jordan," in *Proc. 7th Int. Conf. Knowl. Smart Technol. (KST)*, Chonburi, Thailand, 2015, pp. 149–154.
[21] A. G. Longley, *Prediction of Tropospheric Radio Transmission Loss Over Irregular Terrain: A Computer Method-1968*. Boulder, CO, USA: Inst. Telecommun. Sci., 1968.
[22] (SoftWright LLC, Denver, CO, USA). *Terrain Analysis Package (TAP^{TM})*. (2011). Accessed: Jul. 24, 2023. [Online]. Available: https://www.softwright.com/tap/tap-modules/
[23] H. Kaschel, S. Cordero, and E. Costoya, "Modeling and simulation of the ITM model for point to point prediction on digital television extensible to other technologies," in *Proc. IEEE Int. Conf. Autom./XXIII Congr. Chilean Assoc. Automat. Control (ICA-ACCA)*, 2018, pp. 1–6.
[24] P. L. Rice, *Transmission Loss Predictions for Tropospheric Communication Circuits*, vols. I–II. Boulder, CO, USA: Inst. Telecommun. Sci., 1967.
[25] "Irregular terrain model (ITM) (longley-rice) (20 MHz–20 GHz)." 2020. Accessed: Jul. 24, 2023. [Online]. Available: https://its.ntia.gov/research-topics/radio-propagation-software/itm/itm.aspx
[26] (Cambium Netw., Rolling Meadows, IL, USA). *PTP 550/550e-5 GHz Unlicensed Band Solution Featuring DCS & AES*. Accessed: Jul. 24, 2023. [Online]. Available: https://www.cambiumnetworks.com/products/backhaul/ptp-550/
[27] *Revision of Part 15 of the Commission's Rules to Permit Unlicensed National Information Infrastructure (U-NII) Devices in the 5 GHz Band*, Federal Commun. Comm. (FCC), Washington, DC, USA, 2014.
[28] S. Pérez-Peña et al., "Development of measurement and modeling procedures of diffractive near-LOS wireless links," in *Proc. XXXIIIrd General Assem. Sci. Symp. Int. Union Radio Sci.*, 2020, pp. 1–4.
[29] P. Poshala, K. Rushil, and R. Gupta, *Signal Chain Noise Figure Analysis*, Texas Instrum., Dallas, TX, USA, 2014.
[30] (NXP Semiconduct., Bengaluru, Karnataka). *WLAN 5 GHz Front-End IC*. Accessed Jul. 24, 2023. [Online]. Available: https://www.nxp.com/docs/en/data-sheet/WLAN7001C.pdf
[31] (Skyworks Solut., Irvine, CA, USA). *Dual-Band 802.11A/G/N/Ac Wireless LAN Front End*. Accessed: Jul. 24, 2023. [Online]. Available: https://www.skyworksinc.com/-/media/SkyWorks/Documents/Products/2101–2200/SKY85806_11_203186G.pdf
[32] (Microchip Technol., Chandler, AZ, USA). *4.9–5.9 GHz High-Linearity, High-Efficiency Front-End Module*. Accessed: Jul. 24, 2023. [Online]. Available: https://ww1.microchip.com/downloads/aemDocuments/documents/OTH/ProductDocuments/DataSheets/70005081B.pdf
[33] (Qualcomm, San Diego, CA, USA). *Fully Integrated Wi-Fi Front end Module Designed for Wireless Infrastructure and Networking Applications*. Accessed: Jul. 24, 2023. [Online]. Available: https://www.qualcomm.com/products/technology/modems/rf/qxm80xx
[34] L. Ward, *802.11AC Technology Introduction White Paper*. Munich, Germany: Rhode and Schwarz, 2012.
[35] *IEEE 802.11AC-2013, IEEE Standard for Information Technology–Telecommunications and Information Exchange Between Systems Local and Metropolitan Area Networks–Specific Requirements–Part 11: Wireless LAN Medium Access Control (MAC) and Physical Layer (PHY) Specifications–Amendment 4: Enhancements for Very High Throughput for Operation in Bands below 6 GHz*, IEEE LAN/MAN Stand. Committee, New York, NY, USA, 2013.
[36] C. Handforth, H. Croxson, and G. Cruz, *Closing the Coverage Gap: How Innovation Can Drive Rural Connectivity*, GSMA Connect. Soc., London, U.K., 2019.
[37] M. Fiorani, S. Tombaz, P. Monti, M. Casoni, and L. Wosinska, "Green backhauling for rural areas," in *Proc. Int. Conf. Opt. Netw. Design Model.*, Stockholm, Sweden, 2014, pp. 114–119.
[38] J. Saunders and N. Marshall, *Mobile Backhaul Options Spectrum Analysis and Recommendations*, GSM Assoc., London, U.K., 2018.

MUNEER M. AL-ZUBI (Member, IEEE) received the Ph.D. degree in engineering from the University of Technology Sydney (UTS), Sydney, Australia, in 2020. He worked as a Research Associate with the Center of Excellence for Innovative Projects, Jordan University of Science and Technology from 2020 to 2021. From 2021 to 2022, he was a Postdoctoral Researcher with the Department of Engineering, University of Luxembourg, Luxembourg, and also, he was a Remote Visiting Scholar with the School of Electrical and Data Engineering, UTS. He is currently a Postdoctoral Researcher with the Communication Theory Lab, King Abdullah University of Science and Technology, Saudi Arabia. His research interests lie in the areas of wireless communication, EM waves propagation, and molecular communication.

MOHAMED-SLIM ALOUINI (Fellow, IEEE) received the Ph.D. degree in electrical engineering from the California Institute of Technology, Pasadena, CA, USA, in 1998. He served as a Faculty Member with the University of Minnesota, Minneapolis, MN, USA, then with Texas A&M University at Qatar, Doha, Qatar, before joining the King Abdullah University of Science and Technology, Thuwal, Makkah, Saudi Arabia, as a Professor of Electrical Engineering in 2009. His current research interests include the modeling, design, and performance analysis of wireless communication systems.